coatings

MDPI

Article

Electrochromic Polymers Based on 1,4-Bis((9H-carbazol-9-yl)methyl)benzene and 3,4-Ethylenedioxythiophene Derivatives as Promising Electrodes for Flexible Electrochromic Devices

Chung-Wen Kuo [1], Jui-Cheng Chang [2,3], Yu-Xuan Lin [1], Pei-Ying Lee [2], Tzi-Yi Wu [2,*] and Tsung-Han Ho [1,*]

[1] Department of Chemical and Materials Engineering, National Kaohsiung University of Science and Technology, Kaohsiung 80778, Taiwan; welly@nkust.edu.tw (C.-W.K.); b841018@gmail.com (Y.-X.L.)
[2] Department of Chemical Engineering and Materials Engineering, National Yunlin University of Science and Technology, Yunlin 64002, Taiwan; d700215@gmail.com (J.-C.C.); leepeiying1018@gmail.com (P.-Y.L.)
[3] Bachelor Program in Interdisciplinary Studies, National Yunlin University of Science and Technology, Yunlin 64002, Taiwan
* Correspondence: wuty@gemail.yuntech.edu.tw (T.-Y.W.); thho@nkust.edu.tw (T.-H.H.); Tel.: +886-5-534-2601 (ext. 4626) (T.-Y.W.); +886-7-381-4526 (ext. 15125) (T.-H.H.)

Abstract: A 1,4-bis((9H-carbazol-9-yl)methyl)benzene (DCB)-containing homopolymer (P(DCB)) and four DCB- and ED-derivative (3,4-ethylenedioxythiophene (EDOT) and 3,4-ethylenedioxythiophene-methanol (EDm))-containing copolymers (P(DCB-*co*-ED), P(2DCB-*co*-ED), P(DCB-*co*-EDm), and P(2DCB-*co*-EDm)) were electropolymerized on ITO-polyethylene terephthalate (PET) substrates and their electrochromic performances were studied. DCB displays a lower E_{onset} than that of EDOT and EDm, conjecturing that the biscarbazole-containing DCB group shows a stronger electron-donating property than that of the ED derivatives. The P(2DCB-*co*-ED) film presents slate grey, dark khaki, and dark olive green at 0.0, 1.0, and 1.2 V. Bleaching-to-coloring switching studies of polymers show that P(2DCB-*co*-EDm) shows a high ΔT (31.0% at 725 nm) in solutions. Five dual-layer flexible electrochromic devices (ECDs) based on P(DCB), P(DCB-*co*-ED), P(2DCB-*co*-ED), P(DCB-*co*-EDm), and P(2DCB-*co*-EDm) as the anodic materials and PEDOT-PSS as the cathodic material are constructed. The P(2DCB-*co*-ED)/PEDOT-PSS flexible ECD shows a high ΔT (40.3% at 690 nm) and long-term electrochemical cycling stability, while the P(DCB-*co*-EDm)/PEDOT-PSS ECD shows a high ΔT (39.1% at 640 nm) and short response time ($\leq$1.5 s). These findings offer us a new structural insight for the valuable design of conjugated polymers in high-contrast, flexible ECDs.

Keywords: electrochromic polymer; 3,4-ethylenedioxythiophene; transmittance change; response time; colorful-to-colorless switching; flexible electrochromic device

Citation: Kuo, C.-W.; Chang, J.-C.; Lin, Y.-X.; Lee, P.-Y.; Wu, T.-Y.; Ho, T.-H. Electrochromic Polymers Based on 1,4-Bis((9H-carbazol-9-yl)methyl)benzene and 3,4-Ethylenedioxythiophene Derivatives as Promising Electrodes for Flexible Electrochromic Devices. *Coatings* **2022**, *12*, 646. https://doi.org/10.3390/coatings12050646

Academic Editor: Choongik Kim

Received: 28 March 2022
Accepted: 5 May 2022
Published: 9 May 2022

1. Introduction

Electrochromic materials have attracted notable attention for industry and academia owing to their promising applications on anti-dazzling rear view mirrors, smart glasses, electrochromic sunglasses, sensors, information displays, and memory devices [1–3]. Inorganic transition metal oxides (e.g., NiO, WO_3, and V_2O_5), Prussian blue [PB, iron(III) hexacyanoferrate(II)], organic small molecules, and organic polymers are well-known electrochromic materials [4–6]. Compared to those electrochromic materials, organic conjugated polymers have already attracted increasing interest owing to their satisfied advantages, such as easy solution processability, short switching time, tunable optical properties through structural modifications, and large coloration efficiency [7].

The most common conjugated polymers utilized in optoelectronic devices are polytriphenylamine [8,9], polyaniline [10,11], polycarbazole [12,13], polyimide [14,15], polythiophene [16,17], polyindole [18,19], polyoxadiazole [20], and poly(3,4-ethylenedioxythiophene) (PEDOT) [21]. Among these polymers, polycarbazoles show a high hole transporting mobility and can be oxidized to generate dications and radical cations [22]. Rybakiewicz et al.

published the electrochromic results of a naphthalene diimide core-functionalized polycarbazole (polyCNDI), which changed color from red (0.05 V) to orange (0.75 V) and green (0.95 V) during its oxidizing process. For the reduced process, polyCNDI film changes its color from red (−0.85 V) to brown (−1.15 V). Further polarization of polyCNDI film leads to a change of the color to green (−1.55 V). PolyCNDI shows a high ΔT (35% at 783 nm) during electrochromic switching. Moreover, PEDOT is a bicyclic derivative of polythiophenes and it shows low band gap, excellent transparency in the oxidized state, and high electrical conductivity [23]. Toppare et al. synthesized a carbazole-comprising monomer (M1), and 3,4-ethylenedioxythiophene (EDOT) and M1 were used to electrosynthesize electrochromic polymers (CoP1.5 and CoP1.3) with various feed monomer ratios [24]. CoP1.5 and CoP1.3 displayed various tones of violet colors in their reduced states, and the colors changed to blue upon oxidation. CoP1.3 shows a high ΔT (55% at 1050 nm), while CoP1.5 also displays a high ΔT (45% at 1170 nm). Armstrong et al. published the optical and electrochemical results of PEDOT, poly(EDOT-*co*-EDTM (3,4-ethylenedioxythiophene-methanol)), and PEDTM [25]. PEDTM displayed narrower voltammetric peak width than that of PEDOT. The λ_{max} of reduced PEDTM redshifted slightly at 596 nm, compared to 580 nm observed for neutral PEDOT [26].

On the other hand, classical research works have focused on ECDs using conductive glass as a transparent substrate. Recently, more studies have been devoted to plastic substrates due to their flexibility. Mecerreyes et al. fabricated all-polymeric flexible ECDs, the configuration of which was PET plastic substrate | PEDOT | PEO combined with CF_3SO_3Li | PEDOT | PET plastic substrate [27]. Although the preliminary performances of optical contrast and cycling stability are not good enough, this strategy opens novel avenues in the evolution of flexible ECDs. Wen et al. published the experimental results of a flexible ECD with a configuration of PES((polyethersulfone)-ITO | PANI-PSS | electrolyte | PEDOT-PSS | PES-ITO. This flexible ECD maintained its electrochromic switching properties as it was situated at its bending state [28]. Xu et al. constructed and characterized flexible ECDs based on ITO–PET plastic. Similar to a glass-comprising ECD, the ITO-coated PET plastic-comprising ECD showed a rapid switching time (ca. 0.5 s) and long lifetime (more than 40,000 cycles) [29].

Conjugated polymers can be fabricated several ways, such as using electropolymerization, vapor phase polymerization, and oxidative chemical vapor deposition [30,31]. In this study, a biscarbazole (DCB)-containing homopolymer (P(DCB)) and four DCB- and ED-derivative (3,4-ethylenedioxythiophene (EDOT) and 3,4-ethylenedioxythiophene-methanol (EDm))-based copolymers (P(DCB-*co*-ED), P(2DCB-*co*-ED), P(DCB-*co*-EDm), and P(2DCB-*co*-EDm)) are coated electrochemically on ITO-coated PET plastic substrates. The absorption spectra and switching kinetics of the five DCB-containing electrode materials are investigated. Dual-layer flexible ECDs are constructed using P(DCB), P(DCB-*co*-ED), P(2DCB-*co*-ED), P(DCB-*co*-EDm), and P(2DCB-*co*-EDm) as the anodic polymers and PEDOT-PSS as the cathodic polymer. The absorption spectra, switching kinetics, and electrochemical oxidized and reduced stability of the P(DCB)/PEDOT-PSS, P(DCB-*co*-ED)/PEDOT-PSS, P(2DCB-*co*-ED)/PEDOT-PSS, P(DCB-*co*-EDm)/PEDOT-PSS, and P(2DCB-*co*-EDm)/PEDOT-PSS flexible ECDs are explored in detail.

2. Experimental

2.1. Materials and Electrosynthesis of P(DCB), P(DCB-co-ED), P(2DCB-co-ED), P(DCB-co-EDm), and P(2DCB-co-EDm)

EDm and EDOT were purchased from Tokyo Chemical Industry Co., Ltd (Tokyo, Japan). DCB was prepared according to previous methods [32]. The electrochemical deposition of P(DCB), P(DCB-*co*-ED), P(2DCB-*co*-ED), P(DCB-*co*-EDm), and P(2DCB-*co*-EDm) on ITO–PET substrates was implemented potentiostatically at 1.0 V in a 0.1 M $LiClO_4$/acetonitrile (ACN)/dichloromethane (DCM) (DCM/ACN = 1:1, by volume), and the charge density was 20 mC/cm^2. The feed ratios of DCB, EDOT, and EDm are listed in Table 1.

Table 1. Feed species of polymer electrodes.

Electrodes	Feed Species	Molar Ratios
P(DCB)	2 mM DCB	Neat DCB
P(DCB-*co*-ED)	2 mM DCB + 2 mM EDOT	1:1
P(2DCB-*co*-ED)	2 mM DCB + 1 mM EDOT	2:1
P(DCB-*co*-EDm)	2 mM DCB + 2 mM EDm	1:1
P(2DCB-*co*-EDm)	2 mM DCB + 1 mM EDm	2:1

2.2. Instrumental Characterizations

The electrosynthesis and electrochemical characteristics of the P(DCB), P(DCB-*co*-ED), P(2DCB-*co*-ED), P(DCB-*co*-EDm), and P(2DCB-*co*-EDm) films were carried out using an electrochemical analyzer (CHI627E, CH Instruments, Austin, TX, USA). UV–Vis spectra (JASCO International Co., Ltd., Tokyo, Japan), electrochromic photoimages (JASCO International Co., Ltd., Tokyo, Japan) and the switching results of the P(DCB), P(DCB-*co*-ED), P(2DCB-*co*-ED), P(DCB-*co*-EDm), and P(2DCB-*co*-EDm) films and the P(DCB)/PEDOT-PSS, P(DCB-*co*-ED)/PEDOT-PSS, P(2DCB-*co*-ED)/PEDOT-PSS, P(DCB-*co*-EDm)/PEDOT-PSS, and P(2DCB-*co*-EDm)/PEDOT-PSS flexible ECDs were performed using a UV–Vis spectrophotometer (Jasco V–630) and an electrochemical analyzer (CHI627E).

2.3. Fabrication of Flexible ECDs

Electrolytes were prepared using a solution-cast method. 0.3 g $LiClO_4$, 1.1 g propylene carbonate (PC), and 0.4 g PMMA (M_w = 350,000) were added into 2.5 mL ACN, and the mixture was stirred for 8 h. The solution was cast onto ITO–PET substrates, and the samples were dried at 60 °C for 1 day to eliminate ACN completely [33]. The anodic layers (P(DCB), P(DCB-*co*-ED), P(2DCB-*co*-ED), P(DCB-*co*-EDm), and P(2DCB-*co*-EDm)) were polymerized potentiostatically at 1.0 V on ITO–PET substrates, and the charge density was 13.3 mC cm^{-2}. The PEDOT-PSS polymeric membrane was spin-coated on ITO–PET substrate with a rotational speed of 2000 rpm for 1 min. The cathodic and anodic ITO–PET substrates were isolated using a $LiClO_4$/PC/PMMA composite film. The electrode areas of flexible ECDs were 1.5 cm^2.

3. Results and Discussion

3.1. Electrosynthesis

Figure 1 shows the electrochemical oxidation of DCB, EDOT, and EDm in three electrodes cells. The onset potentials for the electrochemical oxidation (E_{onset}) of DCB, EDOT, and EDm were 0.88, 0.98, and 0.96 V, respectively. DCB displayed a lower E_{onset} than that of EDOT and EDm, implying that the biscarbazole-containg DCB group shows stronger electron-donating property than that of the ED derivatives. Figure 2 displays the electrochemical potentiodynamic curves of P(DCB), P(DCB-*co*-ED), P(2DCB-*co*-ED), P(DCB-*co*-EDm), and P(2DCB-*co*-EDm). As the electrosynthesized CV cycles swept continued, the currents of the redox peaks in Figure 2 increased progressively, verifying that the electrochemical growth of P(DCB), P(DCB-*co*-ED), P(2DCB-*co*-ED), P(DCB-*co*-EDm), and P(2DCB-*co*-EDm) occurred on the ITO–PET substrates [34].

The oxidized peaks of P(DCB), P(DCB-*co*-ED), P(2DCB-*co*-ED), P(DCB-*co*-EDm), and P(2DCB-*co*-EDm) were located at 0.77, 0.72, 0.74, 0.73, and 0.72 V, while the reduced peaks of P(DCB), P(DCB-*co*-ED), P(2DCB-*co*-ED), P(DCB-*co*-EDm), and P(2DCB-*co*-EDm) were located at 0.38, 0.32, 0.36, 0.41, and 0.36 V, respectively. The shapes of CV curves, the potentials of oxidized and reduced peaks for P(DCB-*co*-ED), P(2DCB-*co*-ED), P(DCB-*co*-EDm), and P(2DCB-*co*-EDm), were different to those of P(DCB), verifying that the copolymers (P(DCB-*co*-ED), P(2DCB-*co*-ED), P(DCB-*co*-EDm), and P(2DCB-*co*-EDm)) were deposited electrochemically on the ITO–PET substrates. The proposed polymerization schemes of P(DCB), P(DCB-*co*-ED), P(2DCB-*co*-ED), P(DCB-*co*-EDm), and P(2DCB-*co*-EDm) are shown in Figure 3.

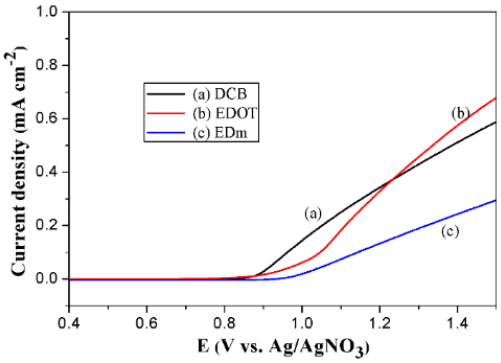

Figure 1. LSV plots of (**a**) 2 mM DCB, (**b**) 2 mM EDOT, and (**c**) 2 mM EDm at 100 mV s^{-1}.

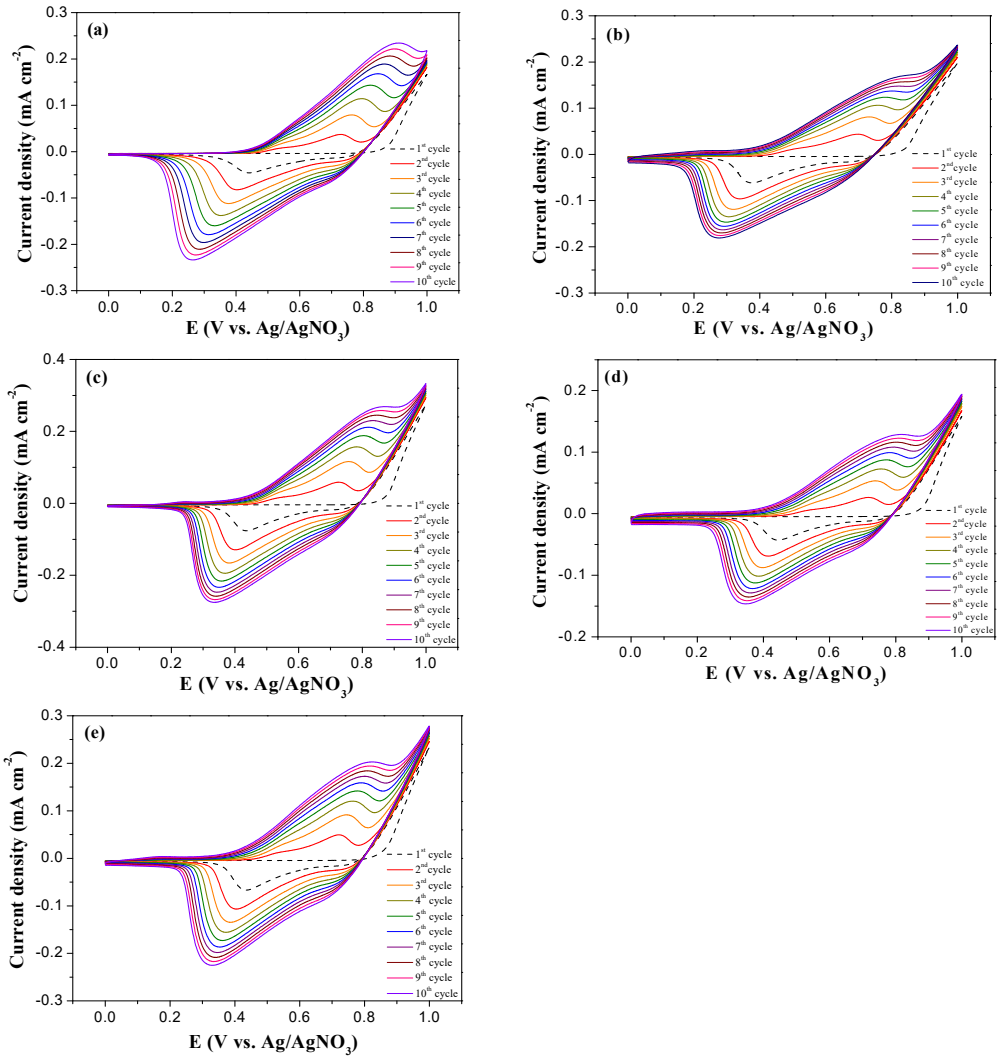

Figure 2. Electrosynthesized plots of (**a**) P(DCB), (**b**) P(DCB-*co*-ED), (**c**) P(2DCB-*co*-ED), (**d**) P(DCB-*co*-EDm), and (**e**) P(2DCB-*co*-EDm). The scan velocity is 100 mV s^{-1}.

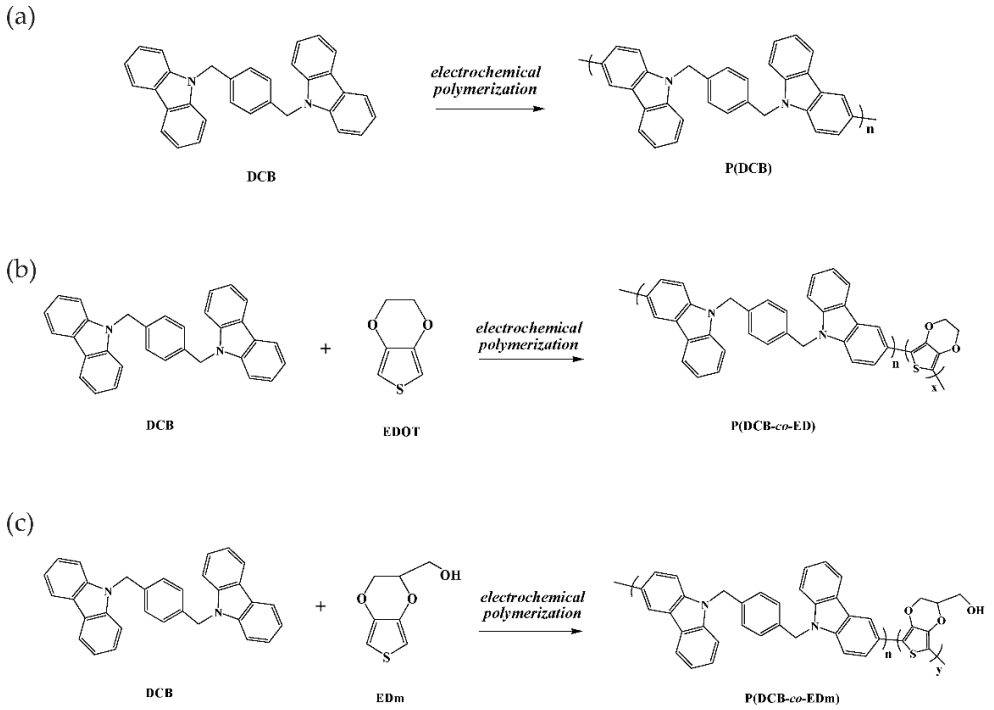

Figure 3. Electrochemical polymerizations of (**a**) P(DCB), (**b**) P(DCB-*co*-ED), and (**c**) P(DCB-*co*-EDm).

Figure 4(a-1)–(e-1) displays the CV plots of the P(DCB), P(DCB-*co*-ED), P(2DCB-*co*-ED), P(DCB-*co*-EDm), and P(2DCB-*co*-EDm) films at different sweep velocities, and Figure 4(a-2)–(e-2) exhibits the relationship figures of currents vs. sweep velocities. The current displays linearity with increasing scan rate, thus we can infer that P(DCB), P(DCB-*co*-ED), P(2DCB-*co*-ED), P(DCB-*co*-EDm), and P(2DCB-*co*-EDm) are affixed to the ITO–PET substrate compactly and the redox actions are non-diffusion controlled [35].

3.2. Spectra and Colour Switching Profiles of P(DCB), P(DCB-co-ED), P(2DCB-co-ED), P(DCB-co-EDm), and P(2DCB-co-EDm)

Figure 5 displays the UV–Vis spectra of P(DCB), P(DCB-*co*-ED), P(2DCB-*co*-ED), P(DCB-*co*-EDm), and P(2DCB-*co*-EDm) at several voltages. There is no conspicuous absorption peak of P(DCB) and PEDOT films at 0.0–0.4 V and at wavelengths of less than 480 nm. When the voltage increases from 0.4 V to 1.1 V, little by little, the absorption bands of Figure 5a appear at 410 and 750 nm, which can be ascribed to the generation of biscarbazole's polarons (or bipolarons) [36]. The absorption peaks of P(DCB), P(DCB-*co*-ED), P(2DCB-*co*-ED), P(DCB-*co*-EDm), and P(2DCB-*co*-EDm) at 0.8 V show two peaks at around 400–450 nm, which can be attributed to the absorption band of biscarbazole groups at an oxidized state and EDOT derivatives at a neutral state. The insets of Figure 5 show the electrochromic photoimages of P(DCB), P(DCB-*co*-ED), P(2DCB-*co*-ED), P(DCB-*co*-EDm), and P(2DCB-*co*-EDm), from bleached to colored state, and the P(DCB) film is light khaki at 0.0 V, olive at 1.0 V, and mustard green at 1.3 V. In an identical situation, the P(DCB-*co*-ED) film reveals light gray at 0.0 V, dim gray at 0.8 V, and moss green at 1.2 V. The P(2DCB-*co*-ED) film is slate grey at 0.0 V, dark khaki at 1.0 V, and dark olive green at 1.2 V. The P(DCB-*co*-EDm) film is gray at 0.0 V, dark khaki at 0.9 V, and dark olive at 1.2 V. The P(2DCB-*co*-EDm) film is light gray at 0.0 V, dim gray at 0.7 V, and olive at 1.0 V. The chromaticity diagrams of P(DCB), P(DCB-*co*-ED), P(2DCB-*co*-ED), P(DCB-*co*-EDm), and P(2DCB-*co*-EDm) monitored at some voltages are summarized in Table 2.

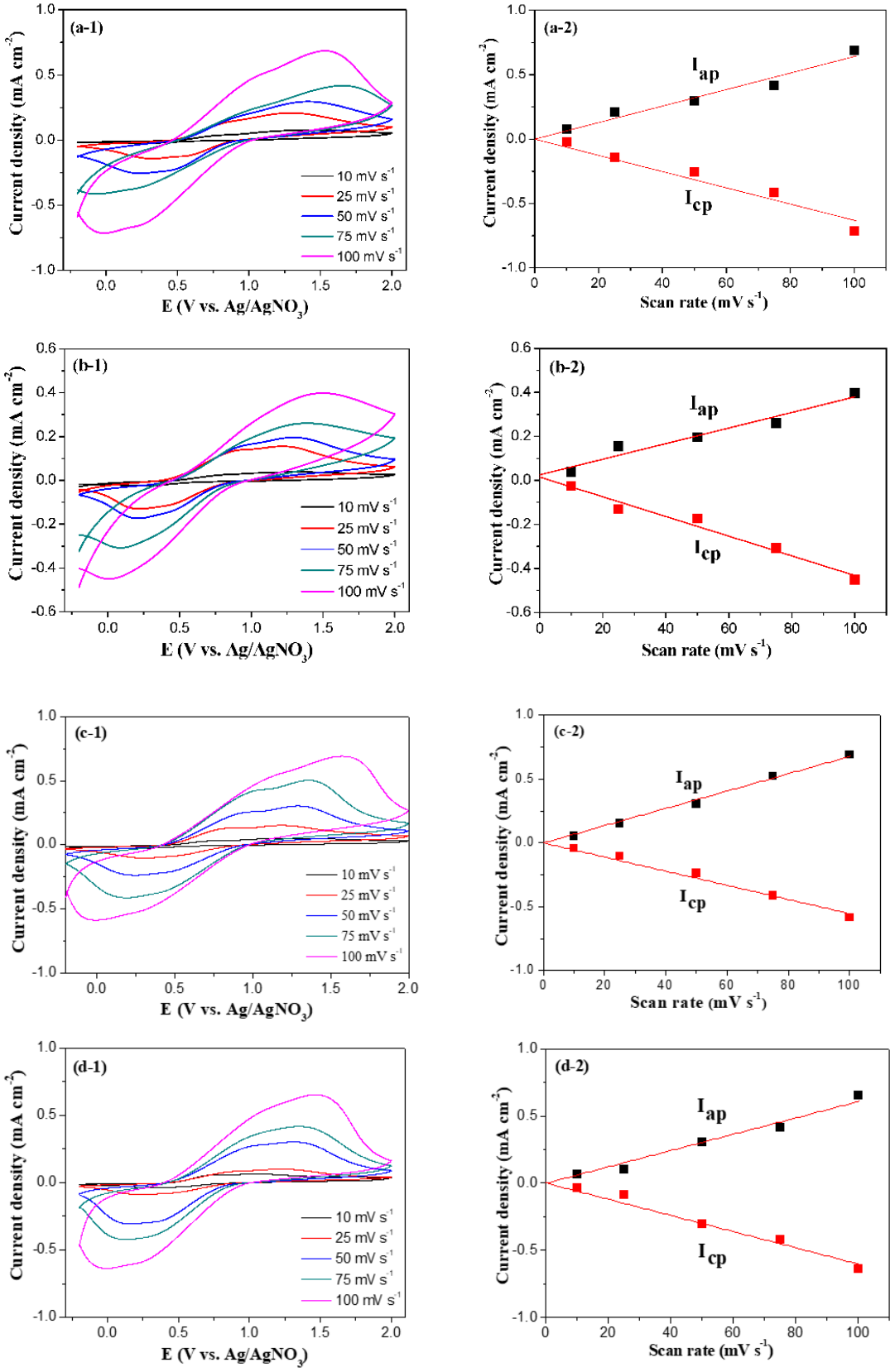

Figure 4. *Cont.*

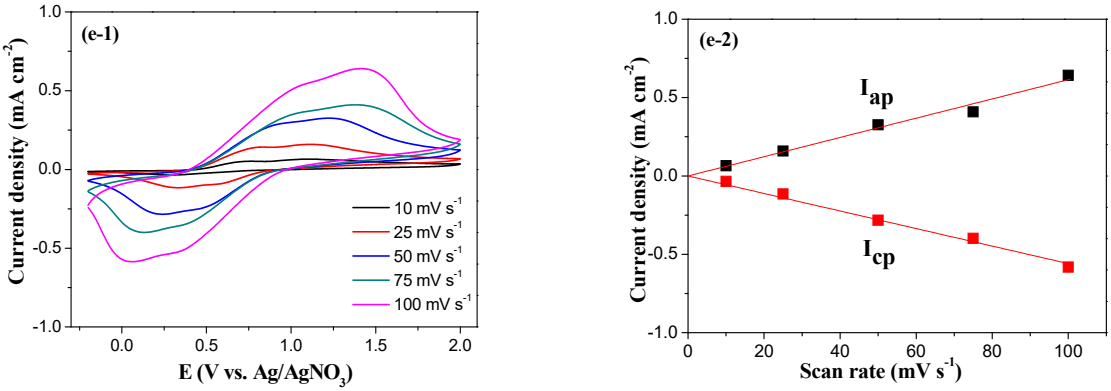

Figure 4. CV curves of (**a-1**) P(DCB), (**b-1**) P(DCB-*co*-ED), (**c-1**) P(2DCB-*co*-ED), (**d-1**) P(DCB-*co*-EDm) and (**e-1**) P(2DCB-*co*-EDm) at different scan rates in a $LiClO_4$/ACN solution. (**a-2**)–(**e-2**) show the dependence of currents on the sweep velocities of polymer membranes.

Table 2. Chromaticity charts of (**a**) P(DCB), (**b**) P(DCB-*co*-ED), (**c**) P(2DCB-*co*-ED), (**d**) P(DCB-*co*-EDm), and (**e**) P(2DCB-*co*-EDm).

Films	*E* (V)	*L** [a]	*a**	*b**	*x*	*y*	Diagrams
(**a**)	0.0	93.92	5.78	10.95	0.3241	0.3538	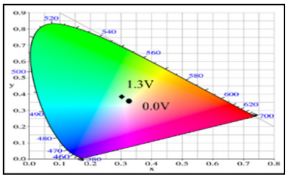
	0.4	94.33	5.24	10.25	0.3236	0.3519	
	0.9	84.40	7.77	30.41	0.3424	0.4085	
	1.0	77.84	−1.24	22.73	0.3234	0.4000	
	1.1	72.61	−2.86	16.44	0.3081	0.3901	
	1.3	69.51	−6.08	12.40	0.3007	0.3808	
(**b**)	0.0	90.11	4.94	7.91	0.3201	0.3480	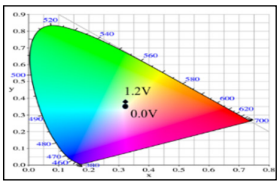
	0.4	91.05	4.12	6.44	0.3186	0.3444	
	0.8	88.36	8.27	17.36	0.3327	0.3701	
	0.9	86.64	9.24	20.24	0.3356	0.3783	
	1.0	83.65	−3.28	19.04	0.3304	0.3793	
	1.2	79.69	−5.63	15.53	0.3203	0.3756	
(**c**)	0.0	93.25	3.19	4.56	0.3164	0.3398	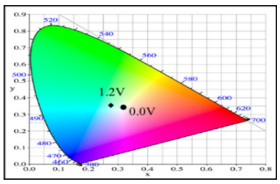
	0.7	88.25	10.68	24.60	0.3421	0.3869	
	0.8	84.94	13.53	26.82	0.3426	0.3963	
	0.9	77.33	10.86	18.11	0.3185	0.3870	
	1.0	67.85	−1.02	6.79	0.2865	0.3673	
	1.2	64.56	−3.99	1.04	0.2745	0.3514	
(**d**)	0.0	93.29	0.03	−0.60	0.3116	0.3279	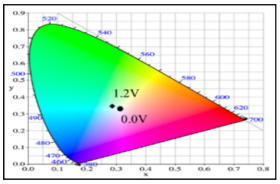
	0.7	90.99	3.58	9.29	0.3245	0.3496	
	0.8	85.55	11.04	21.07	0.3358	0.3815	
	0.9	79.60	15.69	13.06	0.3138	0.3709	
	1.0	72.71	19.13	3.69	0.2882	0.3538	
	1.2	71.99	16.76	0.03	0.2844	0.3427	
(**e**)	0.0	92.92	2.72	3.58	0.3154	0.3376	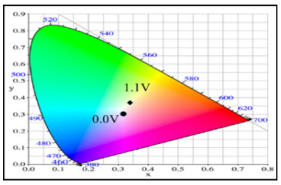
	0.6	90.95	6.08	13.21	0.3280	0.3591	
	0.7	88.02	10.42	23.76	0.3411	0.3851	
	0.8	85.25	13.02	25.02	0.3400	0.3918	
	0.9	79.33	17.39	17.55	0.3198	0.3830	
	1.0	74.17	19.00	8.99	0.2997	0.3665	

[a] ***L**** represents the lightness, ***a**** and ***b**** represent the color channels.

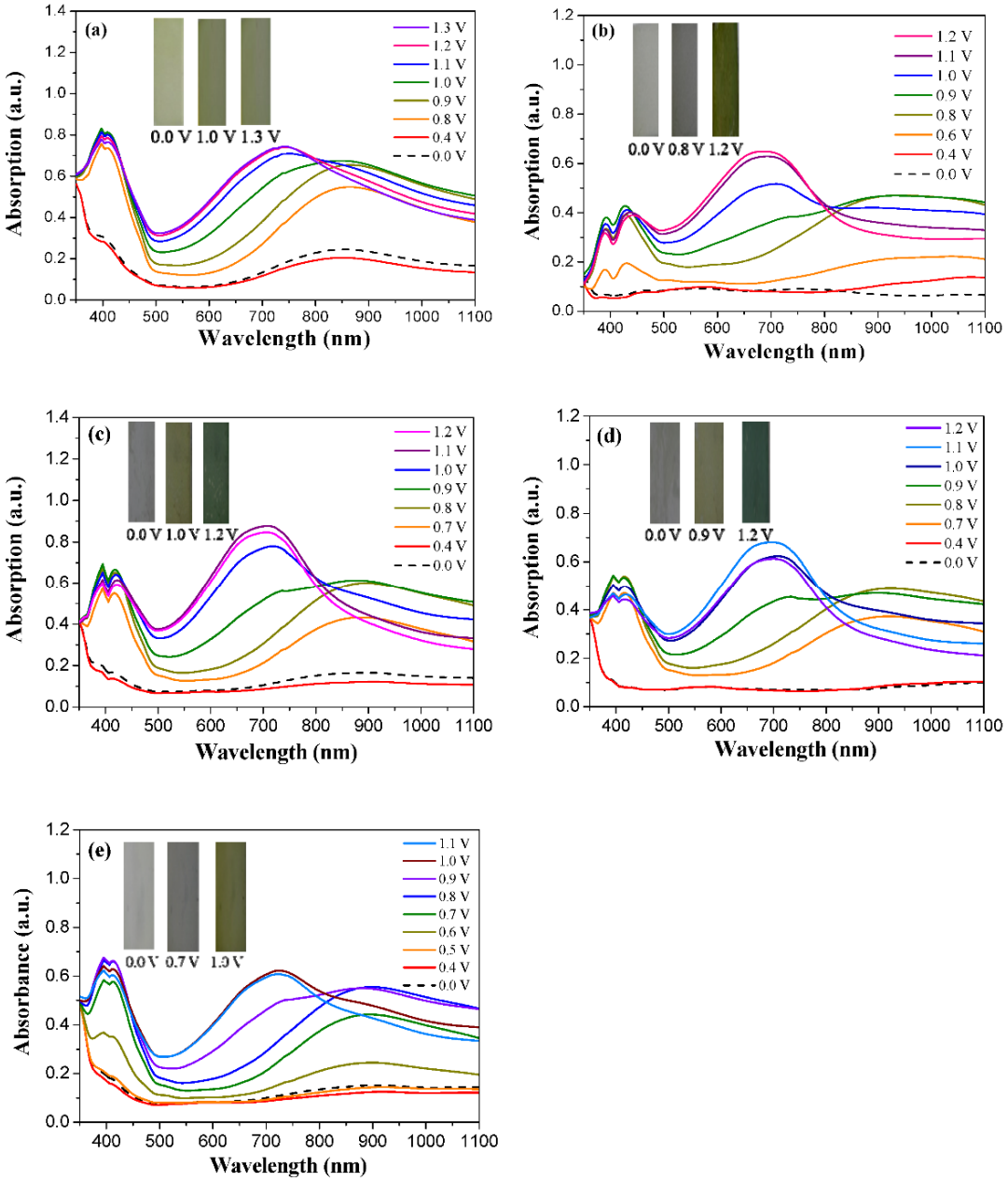

Figure 5. UV–Vis spectra of (**a**) P(DCB), (**b**) P(DCB-*co*-ED), (**c**) P(2DCB-*co*-ED), (**d**) P(DCB-*co*-EDm), and (**e**) P(2DCB-*co*-EDm).

Figure 6 reveals the color-to-colorless switching properties of P(DCB), P(DCB-*co*-ED), P(2DCB-*co*-ED), P(DCB-*co*-EDm), and P(2DCB-*co*-EDm) between +0.4 V and +1.2 V. The time interval is 10 s. The bleached response time (τ_b) and colored response time (τ_c) of P(DCB), P(DCB-*co*-ED), P(2DCB-*co*-ED), P(DCB-*co*-EDm), and P(2DCB-*co*-EDm) are shown in Table 3, and the τ_c and τ_b are calculated at 90% of the entire transmittance variation. The τ_b and τ_c of these polymers at a visible light region were determined to be 2.3–4.9 s in solutions.

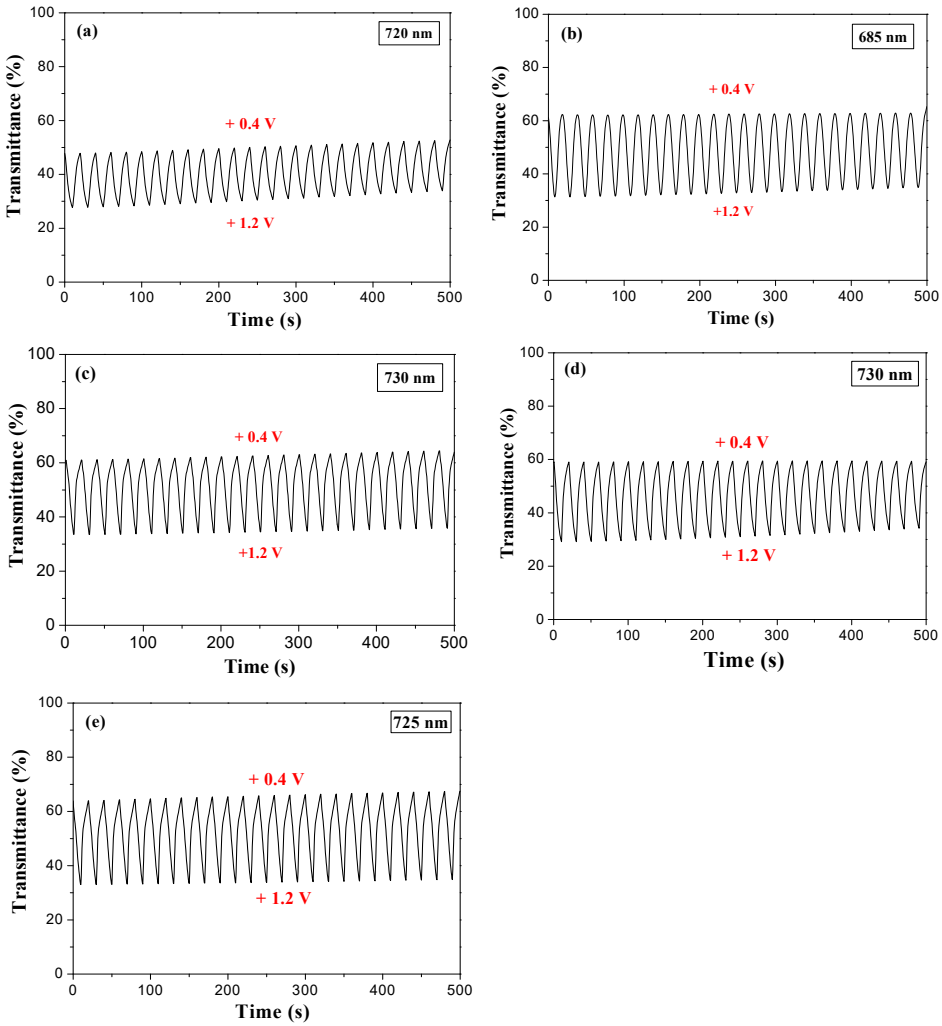

Figure 6. Switching profiles of the (**a**) P(DCB), (**b**) P(DCB-*co*-ED), (**c**) P(2DCB-*co*-ED), (**d**) P(DCB-*co*-EDm), and (**e**) P(2DCB-*co*-EDm) electrodes.

Table 3. Chromic parameters of electrodes.

Electrodes	λ (nm)	T_{ox} (%)	T_{red} (%)	ΔT (%)	ΔOD	Q_d (mC cm^{-2})	η (cm^2 C^{-1})	τ_c (s)	τ_b (s)
P(DCB)	720	28.0	48.0	20.0	0.234	1.880	124.5	3.8	4.9
P(DCB-*co*-ED)	685	31.7	62.2	30.5	0.293	1.859	157.6	3.8	4.0
P(2DCB-*co*-ED)	710	33.5	61.1	27.6	0.261	2.666	97.9	2.3	4.0
P(DCB-*co*-EDm)	730	29.4	59.0	29.7	0.303	1.840	164.7	2.8	4.8
P(2DCB-*co*-EDm)	725	33.2	64.2	31.0	0.287	2.520	113.9	3.1	4.7

The transmittance variations (ΔT) of P(DCB), P(DCB-*co*-ED), P(2DCB-*co*-ED), P(DCB-*co*-EDm), and P(2DCB-*co*-EDm) are 20.0% at 720 nm, 30.5% at 685 nm, 27.6% at 710 nm, 29.7% at 730 nm, and 31.0% at 725 nm, respectively, in solutions. The ED- and EDm-containing polymers display a higher ΔT than that of P(DCB) in a visible light zone. As listed in Table 4, the ΔT of the P(2DCB-*co*-EDm) film is greater than that published for PSNS-F (ΔT = 21.7% at 445 nm) [37], PBDO (ΔT = 24.5% at 610 nm) [38], and PDCP (ΔT = 19% at 1025 nm) [39]. However, the ΔT of the P(2DCB-*co*-EDm) film is lower than that published for P(SNS-PN-*co*-ProDOT) (ΔT = 42% at 850 nm) [40] and PMPS (ΔT = 68.4% at 855 nm) [41].

The variation of optical densities (ΔOD) and coloration efficiencies (η) can be evaluated using two formulas [42], as follows:

$$\Delta OD = \log(T_b/T_c) \quad (1)$$

$$\eta = \Delta OD/Q_d \quad (2)$$

where T_c and T_b indicate the transmittance at colored and bleached states, respectively. The η of P(DCB), P(DCB-*co*-ED), P(2DCB-*co*-ED), P(DCB-*co*-EDm), and P(2DCB-*co*-EDm) is 124.5 cm^2/C at 720 nm, 157.6 cm^2/C at 685 nm, 97.9 cm^2/C at 710 nm, 164.7 cm^2/C at 730 nm, and 113.9 cm^2/C at 725 nm, respectively. P(DCB-*co*-EDm) shows the highest η at 730 nm. The P(DCB) film shows a larger η than that published for PSNS-F (η = 107 cm^2/C at 445 nm) [37], PBDO (η = 75.9 cm^2/C at 610 nm) [38], and PDCP (η = 124 cm^2/C at 1025 nm) [39]. However, the P(DCB) film shows a lower η than that published for P(SNS-PN-*co*-ProDOT) (η = 256 cm^2/C at 850 nm) [40] and PMPS (η = 159.4 cm^2/C at 855 nm) [41].

Table 4. Transmittance changes and coloration efficiencies of polymers (or ECDs).

Polymers or ECDs	ΔT_{max} (%)	η ($cm^2 \cdot C^{-1}$)	E_g (eV)	Ref.
PSNS-F	21.7 (445 nm)	107 (445 nm)	2.18	[37]
PBDO	24.5 (610 nm)	75.9 (610 nm)	2.38	[38]
PDCP	19 (1025 nm)	124 (1025 nm)	2.58	[39]
P(SNS-PN-*co*-ProDOT)	42 (850 nm)	256 (850 nm)	—	[40]
PMPS	68.4 (855 nm)	159.4 (855 nm)	—	[41]
P(DCB)	20 (720 nm)	124.5 (720 nm)	2.48	This work
P(2DCB-*co*-EDm)	31 (725 nm)	113.9 (725 nm)	—	This work
P(SNS-An-Fc-*co*-EDOT)/PEDOT	22 (601 nm)	484 (601 nm)	—	[43]
P(BTC)/PEDOT	26.3 (580 nm)	120 (580 nm)	—	[44]
P(dcb-*co*-cpdt)/PEDOT	39.8 (628 nm)	319.98 (628 nm)	—	[45]
P(ANIL-*co*-TTPA)/PProDOT-Et_2	46.3 (582 nm)	625 (582 nm)	—	[46]
P(DiC-*co*-CDTK)/PEDOT-PSS	38 (635 nm)	634 (635 nm)	—	[39]
P(DCB)/PEDOT-PSS	30.1 (690 nm)	215.9 (690 nm)	—	This work
P(2DCB-*co*-ED)/PEDOT-PSS	40.3 (690 nm)	260 (690 nm)	—	This work

3.3. Spectra and Colour Switching Properties of Flexible ECDs

Flexible ECDs were fabricated using anodically coloring polymers (P(DCB), P(DCB-*co*-ED), P(2DCB-*co*-ED), P(DCB-*co*-EDm), and P(2DCB-*co*-EDm)) and a cathodically coloring polymer (PEDOT-PSS), and their spectra and electrochromic switching figures were determined. As displayed in Figure 7, the P(DCB)/PEDOT-PSS, P(DCB-*co*-ED)/PEDOT-PSS, P(2DCB-*co*-ED)/PEDOT-PSS, P(DCB-*co*-EDm)/PEDOT-PSS, and P(2DCB-*co*-EDm)/PEDOT-PSS ECDs displayed two absorption peaks at around 600–700 nm at 2.0 V, which can be ascribed to the absorption of P(DCB), P(DCB-*co*-ED), P(2DCB-*co*-ED), P(DCB-*co*-EDm), and P(2DCB-*co*-EDm) in an oxidized state and cathodically coloring polymer in a neutral state.

The P(DCB)/PEDOT-PSS ECD was bright gray at −0.5 V, dim gray at 1.2 V, and army blue at 2.0 V. The P(DCB-*co*-ED)/PEDOT-PSS ECD was silver gray at −0.7 V, bright slate gray at 1.2 V, and saxe blue at 2.0 V. The P(2DCB-*co*-ED)/PEDOT-PSS ECD was light gray at −0.5 V, azure at 1.8 V, and Wedgwood blue at 2.0 V. The P(DCB-*co*-EDm)/PEDOT-PSS ECD was Gainsboro gray at −1.0 V, army at 1.6 V, and grayish blue at 2.0 V. The P(2DCB-*co*-EDm)/PEDOT-PSS ECD was slate gray at −1.0 V, gray at 1.6 V, and peacock blue at 2.0 V. The chromaticity diagrams of P(DCB)/PEDOT-PSS, P(DCB-*co*-ED)/PEDOT-PSS, P(2DCB-*co*-ED)/PEDOT-PSS, P(DCB-*co*-EDm)/PEDOT-PSS, and P(2DCB-*co*-EDm)/PEDOT-PSS ECDs at several potentials are shown in Table 5.

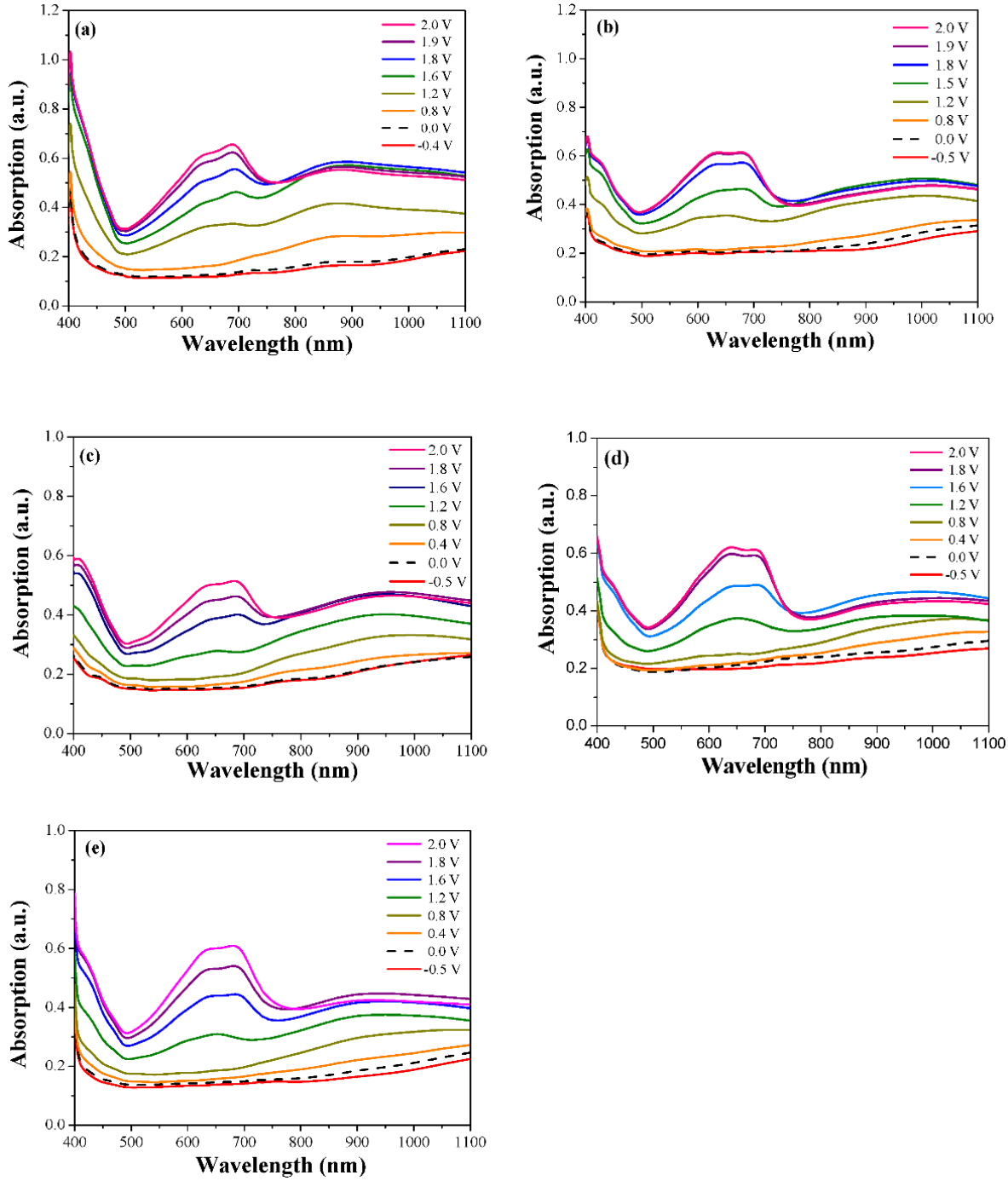

Figure 7. UV–Visible plots of the (**a**) P(DCB)/PEDOT-PSS, (**b**) P(DCB-*co*-ED)/PEDOT-PSS, (**c**) P(2DCB-*co*-ED)/PEDOT-PSS, (**d**) P(DCB-*co*-EDm)/PEDOT-PSS, and (**e**) P(2DCB-*co*-EDm)/PEDOT-PSS devices.

Table 5. Chromaticity diagrams of the (**a**) P(DCB)/PEDOT-PSS, (**b**) P(DCB-*co*-ED)/PEDOT-PSS, (**c**) P(2DCB-*co*-ED)/PEDOT-PSS, (**d**) P(DCB-*co*-EDm)/PEDOT-PSS, and (**e**) P(2DCB-*co*-EDm)/PEDOT-PSS ECDs.

Devices	*E* (V)	Graphs	*L** [a]	*a**	*b**	*x*	*y*	Diagrams
(**a**)	−0.5		90.25	2.84	5.65	0.3190	0.3420	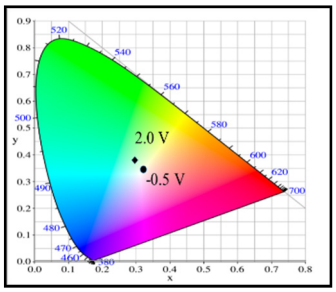
	0.0		89.68	3.17	5.94	0.3191	0.3429	
	1.2		87.34	4.78	8.27	0.3212	0.3491	
	1.6		76.61	17.50	5.60	0.3158	0.3801	
	1.7		75.18	18.75	−4.27	0.3150	0.3838	
	2.0		69.04	22.65	−10.16	0.2948	0.3756	
(**b**)	−0.7		83.91	2.30	3.15	0.3154	0.3372	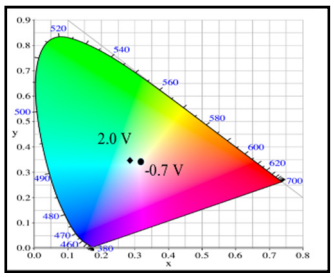
	0.0		83.29	2.13	2.79	0.3150	0.3364	
	0.8		80.78	2.77	4.19	0.3168	0.3401	
	1.2		75.20	7.08	3.16	0.3077	0.3419	
	1.7		68.42	13.34	−3.54	0.2970	0.3495	
	2.0		65.12	15.49	−5.25	0.2837	0.3420	
(**c**)	−0.5		87.58	1.88	3.97	0.3175	0.3383	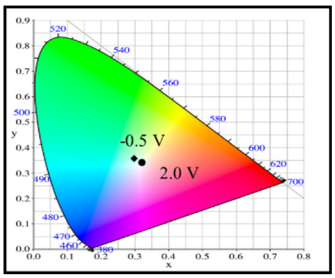
	0.0		87.26	1.96	4.01	0.3174	0.3384	
	0.8		84.79	3.02	5.66	0.3191	0.3429	
	1.6		82.80	4.03	4.79	0.3179	0.3442	
	1.8		75.59	11.98	−6.14	0.3100	0.3577	
	2.0		72.90	13.82	−8.17	0.3025	0.3554	
(**d**)	−1.0		85.73	1.90	1.81	0.3134	0.3340	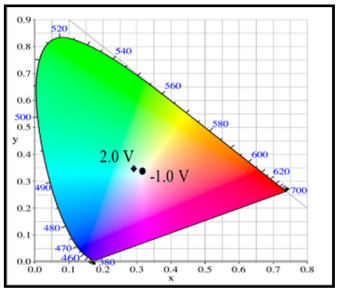
	0.0		86.17	1.72	1.35	0.3128	0.3330	
	1.2		80.27	5.18	3.01	0.3107	0.3395	
	1.6		75.45	10.44	−3.85	0.3036	0.3463	
	1.8		72.16	12.68	−4.09	0.2936	0.3420	
	2.0		70.63	14.04	−5.36	0.2893	0.3415	
(**e**)	−1.0		85.73	1.90	1.81	0.3134	0.3340	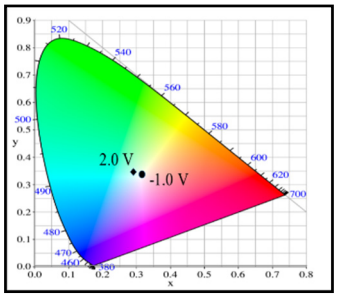
	0.0		86.18	1.76	1.42	0.3128	0.3331	
	1.2		84.37	2.36	2.76	0.3146	0.3364	
	1.6		80.27	5.18	−3.01	0.3107	0.3395	
	1.9		72.16	12.68	−4.09	0.2936	0.3420	
	2.0		70.96	13.72	−7.17	0.2888	0.3399	

[a] ***L**** represents the lightness, ***a**** and ***b**** represent the color channels.

Figure 8 shows the switching plots of the P(DCB)/PEDOT-PSS, P(DCB-*co*-ED)/PEDOT-PSS, P(2DCB-*co*-ED)/PEDOT-PSS, P(DCB-*co*-EDm)/PEDOT-PSS, and P(2DCB-*co*-EDm)/PEDOT-PSS ECDs, and the ΔT, ΔOD, η, and τ of the ECDs are displayed in Table 6.

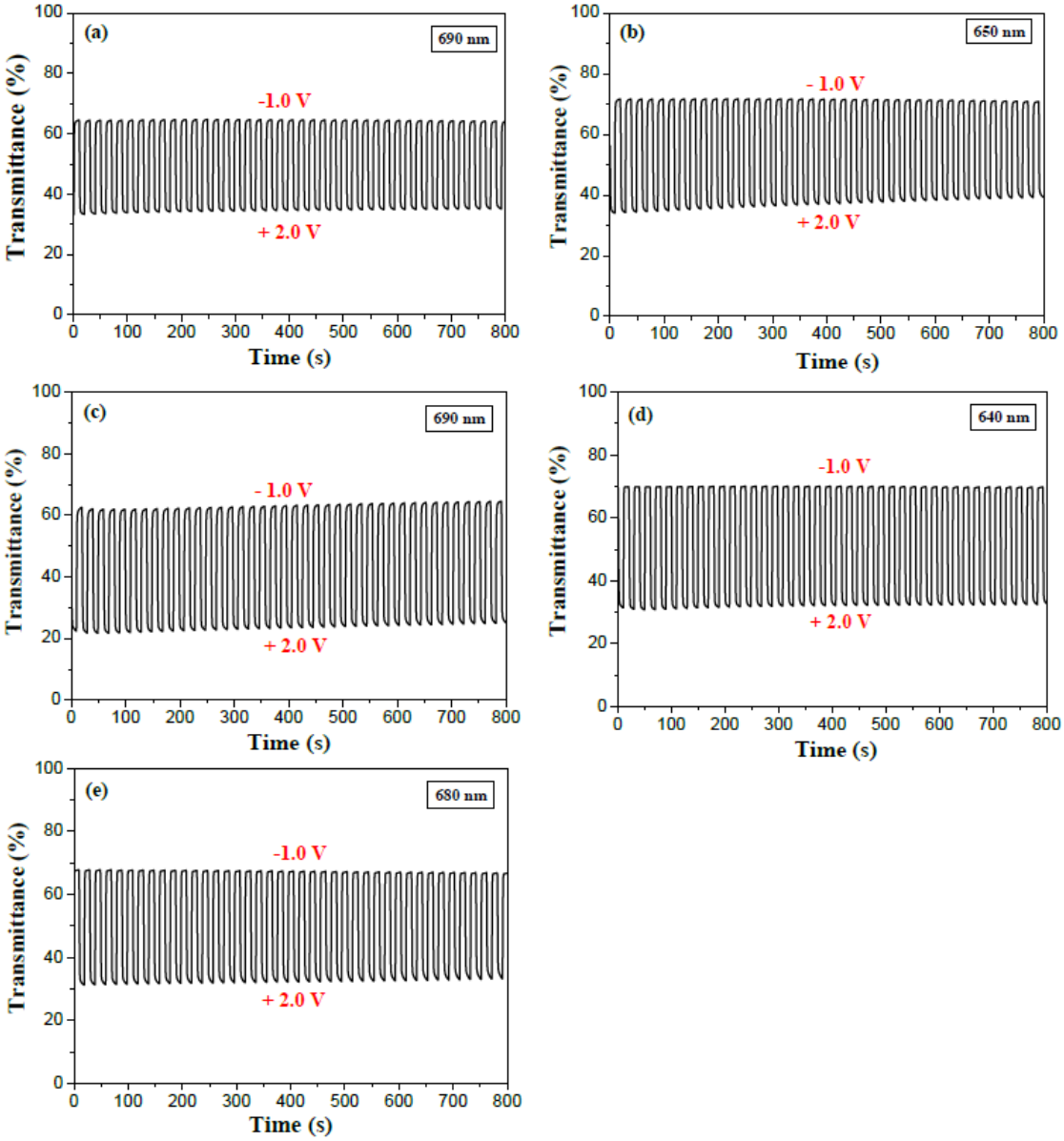

Figure 8. Switching profiles of the (**a**) P(DCB)/PEDOT-PSS, (**b**) P(DCB-*co*-ED)/PEDOT-PSS, (**c**) P(2DCB-*co*-ED)/PEDOT-PSS, (**d**) P(DCB-*co*-EDm)/PEDOT-PSS and (**e**) P(2DCB-*co*-EDm)/PEDOT-PSS devices.

Table 6. Chromic switching parameters of devices.

ECDs	N	T_{ox} (%)	T_{red} (%)	ΔT (%)	ΔOD	Q_d (mC cm^{-2})	η (cm^2 C^{-1})	τ_c (s)	τ_b (s)
P(DCB)/PEDOT-PSS	3	34.4	64.5	30.1	0.27	1.89	215.9	0.4	0.9
(690 nm)	60	35.6	63.4	27.8	0.25	1.81	207.4	1.0	1.1
P(DCB-*co*-ED)/PEDOT-PSS	3	34.5	71.6	37.1	0.32	1.93	245.8	0.2	1.3
(650 nm)	60	39.4	70.8	31.4	0.25	1.70	224.8	0.2	1.1
P(2DCB-*co*-ED)/PEDOT-PSS	3	21.8	62.1	40.3	0.46	2.62	260.0	1.1	1.3
(690 nm)	60	26.0	65.2	39.2	0.40	2.18	275.2	0.9	1.3
P(DCB-*co*-EDm)/PEDOT-PSS	3	30.7	69.8	39.1	0.36	2.69	199.4	1.0	1.5
(640 nm)	60	32.8	69.5	36.7	0.33	2.37	206.3	1.0	1.0
P(2DCB-*co*-EDm)/PEDOT-PSS	3	31.3	67.7	36.4	0.36	2.96	180.2	0.7	1.0
(680 nm)	60	37.3	66.5	29.2	0.25	2.46	153.1	0.4	1.5

The ΔT of the P(DCB)/PEDOT-PSS, P(DCB-*co*-ED)/PEDOT-PSS, P(2DCB-*co*-ED)/PEDOT-PSS, P(DCB-*co*-EDm)/PEDOT-PSS, and P(2DCB-*co*-EDm)/PEDOT-PSS ECDs at the third cycle was 30.1% at 690 nm, 37.1% at 650 nm, 40.3% at 690 nm, 39.1% at 640 nm, and 36.4% at 680 nm, respectively. The ΔT_{max} of the P(2DCB-*co*-ED)/PEDOT-PSS ECD is greater than that of the P(SNS-An-Fc-*co*-EDOT)/PEDOT ECD (ΔT = 22% at 601 nm) [43], P(BTC)/PEDOT ECD (ΔT = 26.3% at 580 nm) [44], P(dcb-*co*-cpdt)/PEDOT ECD (ΔT = 39.8% at 628 nm) [45], and P(DiC-*co*-CDTK)/PEDOT-PSS ECD (ΔT = 38%) [39]. However, the ΔT_{max} of the P(2DCB-*co*-ED)/PEDOT-PSS ECD is lower than that published for the P(ANIL-*co*-TTPA)/PProDOT-Et$_2$ ECD (ΔT = 46.3% at 582 nm) [46]. On the other hand, the η of the P(DCB)/PEDOT-PSS, P(DCB-*co*-ED)/PEDOT-PSS, P(2DCB-*co*-ED)/PEDOT-PSS, P(DCB-*co*-EDm)/PEDOT-PSS, and P(2DCB-*co*-EDm)/PEDOT-PSS ECDs at the third cycle was calculated to be 215.9 cm^2/C at 690 nm, 245.8 cm^2/C at 650 nm, 260.0 cm^2/C at 690 nm, 199.4 cm^2/C at 640 nm, and 180.2 cm^2/C at 680 nm, respectively. The P(2DCB-*co*-ED)/PEDOT-PSS ECD shows a lower η than that published for the P(SNS-An-Fc-*co*-EDOT)/PEDOT ECD (η = 484 cm^2/C at 601 nm) [43], P(dcb-*co*-cpdt)/PEDOT ECD (η = 319.98 cm^2/C at 628 nm) [45], P(ANIL-*co*-TTPA)/PProDOT-Et$_2$ ECD (η = 625 cm^2/C at 582 nm) [46], and P(DiC-*co*-CDTK)/PEDOT-PSS ECD (η = 634 cm^2/C at 635 nm) [39]. This may be attributed to the substrate of the P(2DCB-*co*-ED)/PEDOT-PSS flexible ECD being an ITO-coated PET. Moreover, the τ_b and τ_c of the flexible ECDs calculated at the 3rd and the 60th cycles are shown in Table 6, and they are 0.4–1.5 s. The τ_b and τ_c of the flexible ECDs are faster than those of the polymer electrodes, implying that the distance between two electrodes in flexible ECDs is narrower than those in UV cells [47].

3.4. Redox Stability of Flexible ECDs

The redox stability of five flexible ECDs was monitored using CV in the range of −0.5 V ~ +2.0 V. As displayed in Figure 9, the P(DCB)/PEDOT-PSS, P(DCB-*co*-ED)/PEDOT-PSS, P(2DCB-*co*-ED)/PEDOT-PSS, P(DCB-*co*-EDm)/PEDOT-PSS, and P(2DCB-*co*-EDm)/PEDOT-PSS ECDs showed 96.3%, 96.8%, 97.2%, 91.7%, and 96.6%, respectively, of electroactivity preserved after the 500th cycle, and 90.4%, 95.9%, 96.3%, 79.6%, and 90.1%, respectively, of electroactivity preserved after the 1000th cycle, indicating that the P(DCB)/PEDOT-PSS, P(DCB-*co*-ED)/PEDOT-PSS, P(2DCB-*co*-ED)/PEDOT-PSS, P(DCB-*co*-EDm)/PEDOT-PSS, and P(2DCB-*co*-EDm)/PEDOT-PSS flexible ECDs displayed an adequate long-term redox stability.

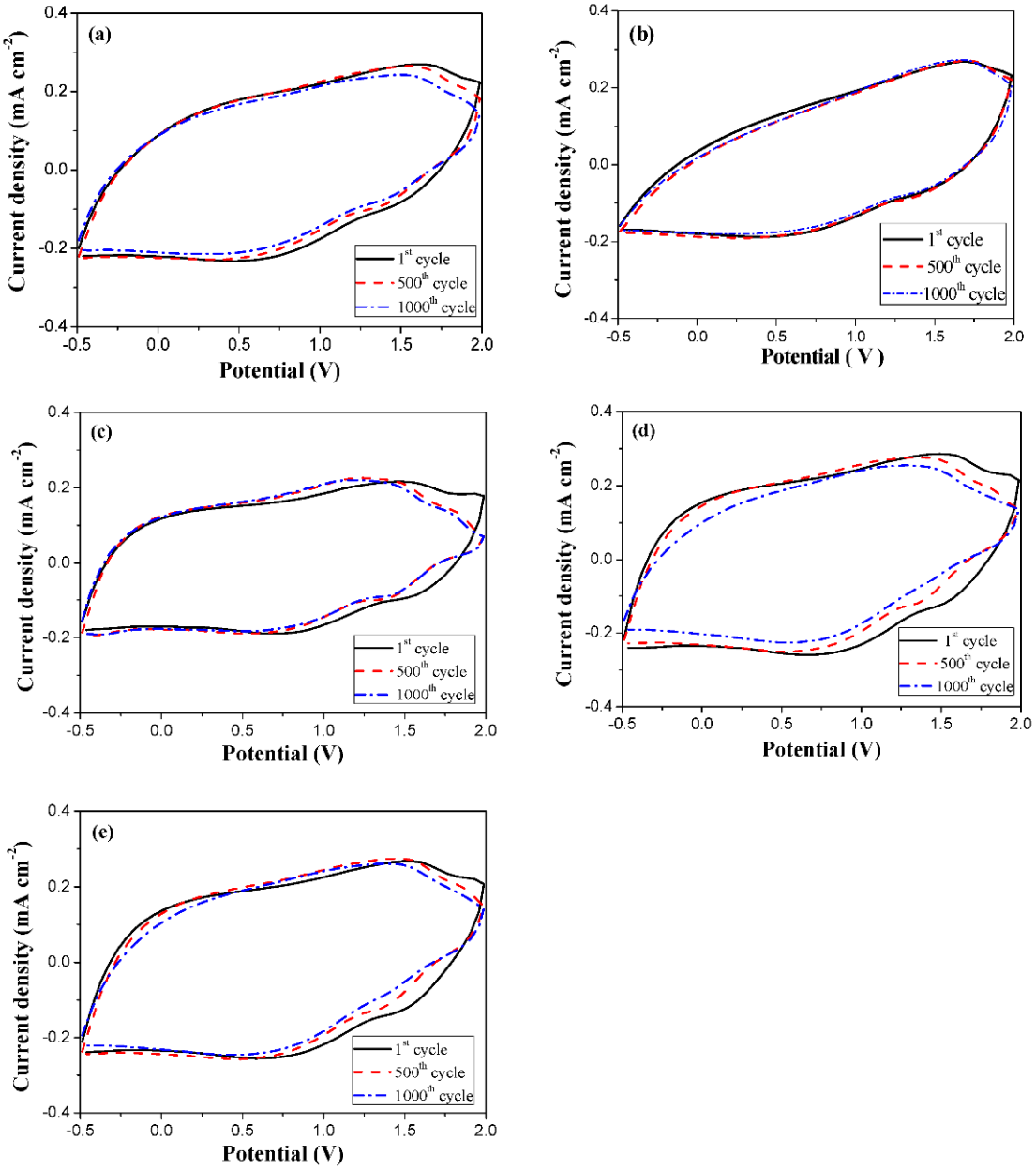

Figure 9. CV curves of the (**a**) P(DCB)/PEDOT-PSS, (**b**) P(DCB-*co*-ED)/PEDOT-PSS, (**c**) P(2DCB-*co*-ED)/PEDOT-PSS, (**d**) P(DCB-*co*-EDm)/PEDOT-PSS and (**e**) P(2DCB-*co*-EDm)/PEDOT-PSS devices.

4. Conclusions

Five biscarbazole-containing anodically coloring polymers (P(DCB), P(DCB-*co*-ED), P(2DCB-*co*-ED), P(DCB-*co*-EDm), and P(2DCB-*co*-EDm)) were electrocoated on ITO coated PET plastic. P(DCB-*co*-EDm) shows three definite color transitions from reduced to oxidized states (gray, dark khaki, and dark olive at 0.0 V, +0.9 V, and +1.2 V, respectively). The spectra and colour switching profiles of the polymeric membranes show that ED- and EDm-containing copolymers have a large ΔT in visible light regions. The dual polymer flexible P(2DCB-*co*-ED)/PEDOT-PSS ECD showed a large ΔT (40.3% at 690 nm) and sufficient redox stability. The P(DCB-*co*-EDm)/PEDOT-PSS ECD displayed a high ΔT (39.1% at 640 nm), rapid electrochromic switching time (less than 1.5 s), and distinct color transitions from Gainsboro gray (at −1.0 V) to army (at 1.6 V). These findings provide avenues for applications of the promising biscarbazole-containing anodically coloring polymers in paper-like, flexible ECDs.

Author Contributions: Conceptualization, C.-W.K.; Data curation, Y.-X.L., P.-Y.L. and T.-Y.W.; Formal analysis, C.-W.K., Y.-X.L., T.-Y.W. and T.-H.H.; Investigation, C.-W.K. and Y.-X.L.; Methodology, C.-W.K., J.-C.C., Y.-X.L. and P.-Y.L.; Resources, J.-C.C. and T.-H.H.; Writing—original draft, C.-W.K., Y.-X.L. and T.-Y.W.; Writing—review & editing, C.-W.K. and T.-Y.W. All authors have read and agreed to the published version of the manuscript.

Funding: This research was funded by the Ministry of Science and Technology of the Republic of China, Grant No. 110-2221-E-992-051 and 108-2221-E-224-049-MY3.

Institutional Review Board Statement: Not applicable.

Informed Consent Statement: Not applicable.

Data Availability Statement: Not applicable.

Conflicts of Interest: The authors declare no conflict of interest.

References

1. Kortz1, C.; Hein, A.; Ciobanu, M.; Walder, L.; Oesterschulze, E. Complementary hybrid electrodes for high contrast electrochromic devices with fast response. *Nat. Commun.* **2019**, *10*, 4874. [CrossRef]
2. Granqvist, C.G.; Arvizu, M.A.; Pehlivan, İ.B.; Qu, H.Y.; Wen, R.T.; Niklasson, G.A. Electrochromic materials and devices for energy efficiency and human comfort in buildings: A critical review. *Electrochim. Acta* **2018**, *259*, 1170–1182. [CrossRef]
3. Cai, G.; Wang, J.; Lee, P.S. Next-generation multifunctional electrochromic devices. *Acc. Chem. Res.* **2016**, *49*, 1469–1476. [CrossRef]
4. Wang, H.; Barrett, M.; Duane, B.; Gu, J.; Zenhausern, F. Materials and processing of polymer-based electrochromic devices. *Mater. Sci. Eng. B* **2018**, *228*, 167–174. [CrossRef]
5. Shchegolkov, A.V.; Jang, S.-H.; Shchegolkov, A.V.; Rodionov, Y.V.; Sukhova, A.O.; Lipkin, M.S. A brief overview of electrochromic materials and related devices: A nanostructured materials perspective. *Nanomaterials* **2021**, *11*, 2376. [CrossRef]
6. Mortimer, R.J. Electrochromic materials. *Annu. Rev. Mater. Res.* **2011**, *41*, 241–268. [CrossRef]
7. Liu, F.H.; Bai, J.; Yu, G.; Ma, F.H.; Hou, Y.J.; Niu, H.J. Synthesis, electrochromic properties and flash memory behaviors of novel D-A-D polyazomethines containing EDOT and thiophene units. *Org. Electron.* **2020**, *77*, 105538. [CrossRef]
8. Sun, T.-G.; Li, Z.-J.; Shao, J.-Y.; Zhong, Y.-W. Electrochromism in electropolymerized films of pyrene-triphenylamine derivatives. *Polymers* **2019**, *11*, 73. [CrossRef]
9. Hsiao, S.H.; Huang, Y.P. Redox-active and fluorescent pyrene-based triarylamine dyes and their derived electrochromic polymers. *Dyes Pigment.* **2018**, *158*, 368–381. [CrossRef]
10. Jamdegni, M.; Kaur, A. Electrochromic behavior of highly stable, flexible electrochromic electrode based on covalently bonded polyaniline-graphene quantum dot composite. *J. Electrochem. Soc.* **2019**, *166*, H502–H509. [CrossRef]
11. Song, S.; Xu, G.; Wang, B.; Gu, J.; Wei, H.; Ren, Z.; Zhang, L.; Zhao, J.; Li, Y. Highly-flexible monolithic integrated infrared electrochromic device based on polyaniline conducting polymer. *Synth. Met.* **2021**, *278*, 116822. [CrossRef]
12. Jiang, M.; Sun, Y.; Ning, J.; Chen, Y.; Wu, Y.; Hu, Z.; Shuja, A.; Meng, H. Diphenyl sulfone based multicolored cathodically coloring electrochromic materials with high contrast. *Org. Electron.* **2020**, *83*, 105741. [CrossRef]
13. Xu, J.; Ji, Q.; Kong, L.; Du, H.; Ju, X.; Zhao, J. Soluble electrochromic polymers incorporating benzoselenadiazole and electron donor units (carbazole or fluorene): Synthesis and electronic-optical properties. *Polymers* **2018**, *10*, 450. [CrossRef]
14. Zheng, R.; Huang, T.; Zhang, Z.; Sun, Z.; Niu, H.; Wang, C.; Wang, W. Novel polyimides containing flexible carbazole blocks with electrochromic and electrofluorescencechromic properties. *RSC Adv.* **2020**, *10*, 6992–7003. [CrossRef]
15. Hsiao, S.H.; Lu, H.Y. Electrosynthesis of aromatic poly(amide-amine) films from triphenylamine-based electroactive compounds for electrochromic applications. *Polymers* **2017**, *9*, 708. [CrossRef]
16. Chen, W.; Ning, J.; Sun, Y.; Zhou, G.; Murtaza, I.; Shuja, A.; He, Y.; Perepichka, I.F.; Meng, H. Thiophene-2,5-diesters as electrochromic materials: The effect of ester groups on the device performance and stability. *Org. Electron.* **2021**, *96*, 106188. [CrossRef]
17. Chernyshev, A.; Acharya, U.; Pfleger, J.; Trhlíková, O.; Zedník, J.; Vohlídal, J. Iron (II) metallo-supramolecular polymers based on thieno[3,2-b]thiophene for electrochromic applications. *Polymers* **2021**, *13*, 362. [CrossRef]
18. Nie, G.M.; Wang, L.; Liu, C.L. High performance electrochromic devices based on a polyindole derivative, poly(1H-benzo[g]indole). *J. Mater. Chem. C* **2015**, *3*, 11318–11325. [CrossRef]
19. Kuo, C.W.; Wu, T.Y.; Fan, S.C. Applications of poly(indole-6-carboxylic acid-*co*-2,2′-bithiophene) films in high-contrast electrochromic devices. *Coatings* **2018**, *8*, 102. [CrossRef]
20. Liu, J.; Shi, Y.; Wu, J.; Li, M.; Zheng, J.; Xu, C. Yellow electrochromic polymer materials with fine tuning electrofluorescences by adjusting steric hindrance of sidechains. *RSC Adv.* **2017**, *7*, 25444–25449. [CrossRef]
21. Shi, J.; Zhu, X.; Xu, P.; Zhu, M.; Guo, Y.; He, Y.; Hu, Z.; Murtaza, I.; Yu, H.; Yan, L.; et al. A redox-dependent electrochromic material: *Tetri*-EDOT substituted thieno[3,2-*b*]thiophene. *Macromol. Rapid Commun.* **2016**, *37*, 1344–1351. [CrossRef] [PubMed]
22. Bekkar, F.; Bettahar, F.; Moreno, I.; Meghabar, R.; Hamadouche, M.; Hernáez, E.; Vilas-Vilela, J.L.; Ruiz-Rubio, L. Polycarbazole and its derivatives: Synthesis and applications. A review of the last 10 years. *Polymers* **2020**, *12*, 2227. [CrossRef] [PubMed]

23. Zhang, L.; Wen, Y.; Yao, Y.; Duan, X.; Xu, J. Electrosynthesis, characterization, and application of poly(3,4-ethylenedioxythiophene) derivative with a chloromethyl functionality. *J. Appl. Polym.* **2013**, *130*, 2660–2670. [CrossRef]
24. Kalay, I.; Yiğit, D.; Güllü, M.; Depci, T.; Toppare, L.; Hacioglu, S.O. Enhancing electrochemical and electrochromic performances of carbazole comprising monomer via copolymerization with 3,4-ethylenedioxythiophene (EDOT). *Synth. Met.* **2020**, *267*, 116449. [CrossRef]
25. Walter, J.D.; Ronald, J.W.; Neal, R.A.; Saavedra, S.S. Electrochemical copolymerization and spectroelectrochemical characterization of 3,4-ethylenedioxythiophene and 3,4-ethylenedioxythiophene−methanol copolymers on Indium−Tin oxide. *Macromolecules* **2006**, *39*, 4418–4424.
26. Akoudad, S.; Roncali, J. Modification of the electrochemical and electronic properties of electrogenerated poly(3,4-ethylenedioxythiophene) by hydroxymethyl and oligo(oxyethylene) substituents. *J. Electrochem. Commun.* **2000**, *2*, 72–76. [CrossRef]
27. Mecerreyes, D.; Marcilla, R.; Ochoteco, E.; Grande, H.; Pomposo, J.A.; Vergaz, R.; Sánchez Pena, J.M. A simplified all-polymer flexible electrochromic device. *Electrochim. Acta* **2004**, *49*, 3555–3559. [CrossRef]
28. Huang, L.-M.; Chen, C.-H.; Wen, T.-C. Development and characterization of flexible electrochromic devices based on polyaniline and poly(3,4-ethylenedioxythiophene)-poly(styrene sulfonic acid). *Electrochim. Acta* **2006**, *51*, 5858–5863. [CrossRef]
29. Ma, C.; Taya, M.; Xu, C. Flexible electrochromic device based on poly(3,4-(2,2-dimethylpropylenedioxy)thiophene). *Electrochim. Acta* **2008**, *54*, 598–605. [CrossRef]
30. Brooke, R.; Edberg, J.; Crispin, X.; Berggren, M.; Engquist, I.; Jonsson, M.P. Greyscale and paper electrochromic polymer displays by UV patterning. *Polymers* **2019**, *11*, 267. [CrossRef]
31. Gharahcheshmeh, M.H.; Gleason, K.K. Device fabrication based on oxidative chemical vapor deposition (oCVD) synthesis of conducting polymers and related conjugated organic materials. *Adv. Mater. Interfaces.* **2019**, *6*, 1801564. [CrossRef]
32. Kuo, C.-W.; Chang, J.-C.; Lee, L.-T.; Lin, Y.-D.; Lee, P.-Y.; Wu, T.-Y. 1,4-Bis((9H-Carbazol-9-yl)methyl)benzene-containing electrochromic polymers as potential electrodes for high-contrast electrochromic devices. *Polymers* **2022**, *14*, 1175. [CrossRef] [PubMed]
33. Kuo, C.W.; Chen, B.K.; Li, W.B.; Tseng, L.Y.; Wu, T.Y.; Tseng, C.G.; Chen, H.R.; Huang, Y.C. Effects of supporting electrolytes on spectroelectrochemical and electrochromic properties of polyaniline-poly(styrene sulfonic acid) and poly(ethylenedioxythiophene)-poly(styrene sulfonic acid)-based electrochromic device. *J. Chin. Chem. Soc.* **2014**, *61*, 563–570. [CrossRef]
34. Idzik, K.R.; Frydel, J.; Beckert, R.; Ledwon, P.; Lapkowski, M.; Fasting, C.; Müller, C.; Licha, T. Synthesis and electrochemical properties of tetrathienyl-linked branched polymers with various aromatic cores. *Electrochim. Acta* **2012**, *79*, 154–161. [CrossRef]
35. Soganci, T. Effects of *N*-substitution group on electrochemical, electrochromic and optical properties of dithienyl derivative. *J. Electrochem. Soc.* **2019**, *166*, H12–H18. [CrossRef]
36. Wu, T.Y.; Tung, Y.H. Phenylthiophene-containing poly(2,5-dithienylpyrrole)s as potential anodic layers for high-contrast electrochromic devices. *J. Electrochem. Soc.* **2018**, *165*, H183–H195. [CrossRef]
37. Cihaner, A.; Algi, F. Processable electrochromic and fluorescent polymers based on *N*-substituted thienylpyrrole. *Electrochim. Acta* **2008**, *54*, 665–670. [CrossRef]
38. Wu, T.-Y.; Su, Y.-S. Electrochemical synthesis and characterization of 1,4-benzodioxan-based electrochromic polymer and its application in electrochromic devices. *J. Electrochem. Soc.* **2015**, *162*, G103–G112. [CrossRef]
39. Kuo, C.W.; Wu, B.W.; Chang, J.K.; Chang, J.C.; Lee, L.T.; Wu, T.Y.; Ho, T.H. Electrochromic devices based on poly(2,6-di(9H-carbazol-9-yl)pyridine)-type polymer films and PEDOT-PSS. *Polymers* **2018**, *10*, 604. [CrossRef]
40. Bingol, B.E.; Tekin, B.; Carbas, B.B. An investigation on electrochromic properties of new copolymers based on dithienylpyrrole and propylenedioxythiophene. *J. Electroanal. Chem.* **2017**, *806*, 107–115. [CrossRef]
41. Kuo, C.W.; Chang, J.C.; Chang, J.K.; Huang, S.W.; Lee, P.Y.; Wu, T.Y. Electrosynthesis of electrochromic polymer membranes based on 3,6-di(2-thienyl)carbazole and thiophene derivatives. *Membranes* **2021**, *11*, 125. [CrossRef] [PubMed]
42. Zhang, Y.; Kong, L.; Zhang, Y.; Du, H.; Zhao, J.; Chen, S.; Xie, Y.; Wang, Y. Ultra-low-band gap thienoisoindigo-based ambipolar type neutral green copolymers with ProDOT and thiophene units as NIR electrochromic materials. *Org. Electron.* **2020**, *81*, 105685. [CrossRef]
43. Camurlu, P.; Gültekin, C. A comprehensive study on utilization of *N*-substituted poly(2,5-dithienylpyrrole) derivatives in electrochromic devices. *Sol. Energy Mater. Sol. Cells* **2012**, *107*, 142–147. [CrossRef]
44. Kong, L.; Wang, Z.; Zhao, J.S.; Xu, J.Z. Multi-electrochromic 2,7-linked polycarbazole derivative and its application in electrochromic devices. *Int. J. Electrochem. Sci.* **2015**, *10*, 982–996.
45. Chen, S.; Gao, Q.; Zhao, J.; Cui, C.; Yang, W.; Zhang, X. Electrosynthesis, characterizations and electrochromic properties of a novel copolymer of 4,4′-di(*N*-carbazoyl)biphenyl with 4H-cyclopenta[2,1-b:3,4-b′]dithiophene. *Int. J. Electrochem. Sci.* **2012**, *7*, 5256–5272.
46. Wu, T.-Y.; Su, Y.-S.; Chang, J.-C. Dithienylpyrrole- and tris[4-(2-thienyl)phenyl]amine-containing copolymers as promising anodic layers in high-contrast electrochromic devices. *Coatings* **2018**, *8*, 164. [CrossRef]
47. Kuo, C.W.; Chang, J.K.; Lin, Y.C.; Wu, T.Y.; Lee, P.Y.; Ho, T.H. Poly(tris(4-carbazoyl-9-ylphenyl)amine)/three poly(3,4-ethylenedioxythiophene) derivatives in complementary high-contrast electrochromic devices. *Polymers* **2017**, *9*, 543. [CrossRef]